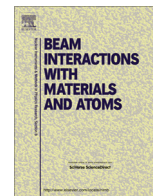




Contents lists available at ScienceDirect

Nuclear Instruments and Methods in Physics Research B

journal homepage: www.elsevier.com/locate/nimb

Investigation of active interrogation techniques to detect special nuclear material in maritime environments: Boarded search of a cargo container ship



Brandon R. Grogan*, James J. Henkel, Jeffrey O. Johnson, John T. Mihalczo, Thomas M. Miller, Bruce W. Patton

Oak Ridge National Laboratory, P.O. Box 2008, Oak Ridge, TN 37831, USA

ARTICLE INFO

Article history:

Received 11 June 2012

Received in revised form 2 July 2013

Available online 29 August 2013

Keywords:

Active interrogation
Special nuclear material
Monte Carlo
Boarded search
Cargo container

ABSTRACT

The detonation of a terrorist nuclear weapon in the United States would result in the massive loss of life and grave economic damage. Even if a device was not detonated, its known or suspected presence aboard a cargo container ship in a U.S. port would have major economic and political consequences. One possible means to prevent this threat would be to board a ship at sea and search for the device before it reaches port. The scenario considered here involves a small Coast Guard team with strong intelligence boarding a container ship to search for a nuclear device. Using active interrogation, the team would nonintrusively search a block of shipping containers to locate the fissile material. Potential interrogation source and detector technologies for the team are discussed. The methodology of the scan is presented along with a technique for calculating the required interrogation source strength using computer simulations. MCNPX was used to construct a computer model of a container ship, and several search scenarios were simulated. The results of the simulations are presented in terms of the source strength required for each interrogation scenario. Validation measurements were performed in order to scale these simulation results to expected performance. Interrogations through the short (2.4 m) axis of a standardized shipping container appear to be feasible given the entire range of container loadings tested. Interrogations through several containers at once or a single container through its long (12.2 m) axis do not appear to be viable with a portable interrogation system.

© 2013 Elsevier B.V. All rights reserved.

1. Introduction

The possibility of a nuclear weapon being smuggled into the United States by terrorists poses a grave threat to the country. Studies estimate that a 10 kiloton nuclear weapon detonated in a major U.S. city could kill up to 500,000 people and do more than \$1 trillion in economic damage [1,2]. Even if a device was not detonated, but known or suspected to be aboard a cargo container ship in a U.S. port, shutting down a major port to search for it could cost billions of dollars per day [1].

Each year, more than 11 million standardized shipping containers arrive in the United States [3], making them a possible conveyance for a nuclear weapon being smuggled by terrorists. Since the World Trade Center attacks of 2001, radiation portal monitors (RPMs) have been installed in U.S. ports [4] and in most foreign ports where goods depart for the United States [5]. Additionally, systems that actively scan a container have been developed. These

systems seek to increase the detector signal produced by special nuclear material (SNM) by inducing fissions with radiation. This technique is known as active interrogation. Refs. [6–8] present some examples of those technologies. If the portals or the active scan indicate the presence of SNM, Customs and Border Patrol agents with handheld radiation detectors could then open the cargo container and inspect the contents manually. While these methods could potentially detect a nuclear weapon once it has already reached port, it is clearly beneficial to detect it as far from the destination port as possible. If intelligence suggests that a nuclear bomb is onboard a container ship after it has already departed for the United States, one likely scenario would be for the U.S. Coast Guard to board the ship and attempt to locate the device while still at sea.

2. The boarded search

This paper will consider the use of active interrogation to locate a nuclear device or a significant quantity of SNM onboard a container ship at sea. There is assumed to be intelligence that limits

* Corresponding author. Tel.: +1 865 576 7468; fax: +1 865 574 9619.
E-mail address: groganbr@ornl.gov (B.R. Grogan).

the number of containers to be searched based on factors such as the shipping company or country of origin. Without this information, a search could still be conducted, but the time required would be greatly increased. A small search team would board the ship from a Coast Guard vessel and conduct a search of the area of interest container by container. The equipment will have to be light enough to be carried by hand and small enough to fit into the access hatches into the ships holds. For this work, it is assumed that no piece of equipment may weigh over 50 lbs (22.7 kg).

Because of the 50 lb weight limit, large accelerator-driven sources could not be used. The heavy shielding that would be required to protect the boarding crew from radiation makes radionuclide sources such as ^{252}Cf or ^{60}Co unsuitable as well. The source selected for the boarded search simulations is a deuterium–tritium (D–T) neutron generator. The D–T neutron generator produces 14.1 MeV neutrons via the $^3\text{H}(^2\text{H}, n)^4\text{He}$ reaction. These neutrons have a higher energy and thus greater penetrating power in most materials than competing technologies such as a deuterium–deuterium (D–D) generator. Commercial D–T neutron generators weighing 50 lb or less are available [9], and have already been employed in portable active interrogation systems [10]. The source is assumed to produce neutrons in a series of isotropic neutron pulses.

For the radiation detector, a single 1 m² detector was assumed for the sake of simplicity. This size was chosen so that the results could easily be scaled to a specific detector size by accounting for the change in solid angle. Two common types of detectors were considered for this work. The first is a detector that is sensitive to neutrons of all energies, but not to gamma rays. An example of this type of detector would be a moderated ^3He detector. Thermalized neutrons are detected via the $^3\text{He}(n,p)^3\text{H}$ reaction [11]. With a polyethylene moderator surrounding the ^3He gas, such a detector has a fairly uniform response to neutrons of all energies [12]. Alternate neutron detectors, such as those based on ^6Li or ^{10}B , could be used instead if ^3He detectors are unavailable due to the current shortage [13]. The other type of detector that was considered detects fast neutrons via proton recoil and gamma rays via Compton scattering [11]. An example of this type of detector is an organic scintillator. The neutron energy threshold in the scintillator can be adjusted with the use of a discriminator. A 1 MeV neutron threshold in a typical organic scintillator corresponds to a gamma ray threshold of approximately 160 keV [14]. Some organic materials, such as the Eljen Technology EJ-309 liquid scintillator [15] allow for the use of pulse shape discrimination (PSD) to distinguish between neutrons and photons. Note that neither the detectors nor the D–T source are necessarily the optimal solutions for the boarded search, but rather they were chosen as a starting point given their ready commercial availability. Future work to optimize the source and detectors would be necessary before deploying an actual system.

For the search, the active interrogation source was assumed to be on one side of a shipping container and the detector on the other. That configuration would minimize the number of interrogating particles traveling directly to the detector during each pulse, which would minimize the detector recovery time after each pulse. Onboard many container ships, the spaces between containers will be too small to place equipment, and access to them may be very difficult; however, for this work it was assumed that there was sufficient space in order to test the physics of detection.

The presence of fissile material would be determined by measuring the number of counts occurring in a region of interest (ROI) after each neutron pulse. The ROI would begin at some time after the pulse to allow for the interrogating radiation to die away and then end before the start of the next pulse. The sum of the ROI counts for all pulses during the interrogation time at a particular location would be used to determine the total response. Because

the interrogating radiation would induce fission chains in fissile material, a larger response should be observed during the interrogation period than from the container cargo material alone. For this work, the difference between the detector response with and without SNM was used to calculate the net strength of the SNM response. Note that in an actual search, it would not be possible to measure an identical container with and without the fissile material. In this case, an estimate of the worst case background across a wide range of cargos would have to be developed instead. Developing such an estimate was beyond the scope of this work, and was not considered further.

In a previous paper [16] it was shown that the required source strength (in particles per second) to detect fissile material for this scenario is

$$N = \frac{z^2 B_A + \sqrt{z^4 B_A^2 + 4z^2 \Delta^2 B_N}}{2T\Delta^2} \quad (1)$$

where T is the interrogation time, B_A is the active background, Δ is the additional HEU signal in the detector per interrogating particle, B_N is the passive background rate due to cosmic rays and natural radioactive sources, and z is the desired detection threshold (in standard deviation) above the total (active + passive) background. Note that when the SNM is heavily shielded, it is expected that $B_A \gg \Delta$. In this circumstance, Equation 1 reduces to

$$N = \frac{z^2 B_A}{T\Delta^2}. \quad (2)$$

The most important implication of Eq. 2 is that the required source strength (N) is proportional to the square of the statistical significance (z^2) when this condition is met.

3. Modeling and simulation

Because the location of the threat object in this scenario is limited to a particular block of containers, only a section representative of a single cargo hold of a container ship was modeled. The modeled section consists of a 38 m length (fore to aft) of double hull wrapped around a block of standardized shipping containers. Each container has 0.3 cm Cor-Ten steel walls and measures 12.2 m long by 2.4 m wide by 2.6 m high. The containers are filled with a homogenous cargo of iron, polyethylene, or a mixture of the two at densities of 0.2, 0.4, or 0.6 g/cm³. 12.2 m long containers are limited to approximately 0.4 g/cm³ because of regulations on the overall weight [17]; however, the shorter 6.1 m long containers can reach average densities of just over 0.6 g/cm³. These shorter containers are often intermixed with the longer ones onboard a cargo ship. Thus, these densities represent light, medium, and heavy cargo loadings that might be encountered in a typical row of containers. Homogeneous cargo was used for simplicity of modeling and also as a conservative estimate because a previous study showed that the presence of particle streaming paths in the cargo makes detection easier [18]. There is a 15.24 cm air gap between containers. One block of containers is below the main deck, and another is on top. Each block is 3 containers deep, 10 wide, and 6 high. In total, the section consists of 360 containers. A medium-sized container ship might carry 1800 to 2160 containers in 5 or 6 holds of this type. Fig. 1 shows the layout of the modeled section.

Figure 2 shows the modeled configurations of source, detector, and threat object within a block of containers. The threat object is represented by a 25 kg sphere of 93% enriched HEU, a “significant quantity” as defined by the International Atomic Energy Agency [19]. Because weapons-grade plutonium produces approximately 10,000 times the passive neutron signal of HEU [12], it is much easier to detect passively and was not considered here. The HEU sphere is located at the center of a cargo container near the center

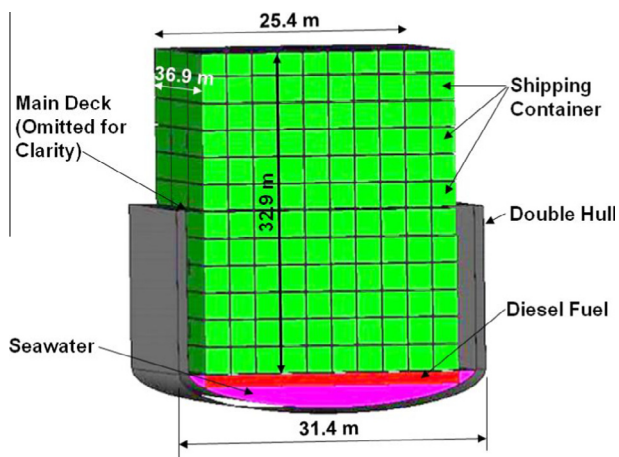


Fig. 1. The container ship model. The model represents a 38 m long (fore to aft) section of a container ship. It contains two blocks of standard 12.2 m shipping containers stacked three deep, six high, and ten wide. The main deck between the two blocks has been omitted for clarity.

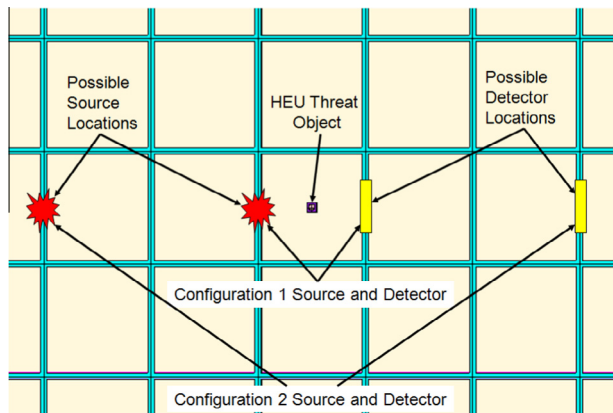


Fig. 2. A cross section of the container array containing the HEU threat object. The view is perpendicular to the long axes of the containers. The two source and detector configurations modeled in the simulations are shown.

of the container array. It is inside an aluminum box filled with balsa wood. The aluminum box is a cube with 22.9 cm sides and 0.32 cm thick walls. The box is meant to represent a generic carrying case that might be used for transporting equipment, and the dimensions are not based on any specific design. The source and detectors are located in gaps between containers with the threat object directly between them.

Two source-detector configurations were considered. In the first configuration, the interrogation source and detector are located directly adjacent to the container with the threat object. In the second configuration, both the source and the detector are moved two containers farther away from the one with the threat object. The second configuration is used to investigate the relative difficulty of scanning several containers at once. This distance is also equivalent to the long axis of a 40' (12.2 m) container.

The MCNPX model uses a 1 m × 1 m × 5 cm rectangular parallelepiped for the detector cell. All particles above the cutoff energy (160 keV for gammas, none for neutrons) crossing into the front face of the detector were tallied by an F1 surface current tally. The neutron tally was divided into energy bins of 0 to 1 MeV and >1 MeV. Each tally was divided into time bins beginning at a few nanoseconds wide and becoming progressively wider at longer time lags. The neutron detector tally results were constructed from the total neutron tally across all energies. The fast neutron /gamma

detector was constructed by summing the >1 MeV neutron and gamma tallies. For simplicity, these two tally results will be referred to as the ^3He and scintillator tallies, respectively. The D-T generator was modeled as an isotropic point source of monoenergetic 14.1 MeV neutrons. No pulse width was assumed during the simulations so all source particles were started at $t = 0$. Instead, the pulse width was simulated by convolving it with the tally results during post-processing. This procedure was used so that the different pulse widths could be tested using the same set of tally results.

Simulations were run using the MCNPX 2.6.0 code [20]. The ADVANTG code [21] was used to generate weight windows for variance reduction in order to speed up simulations. For each scenario, a four-step procedure was used. In the first step, the container was interrogated with the D-T source, and the photon and neutron fluence exiting the HEU were tallied into time and energy bins. In the second step, these fluences were used as a source term to simulate induced neutrons and photons exiting the HEU and travelling to the detector. The third step accounted for the portions of the cargo outside of the HEU box and, the fourth simulated the active background by removing the HEU from the simulation. Breaking the simulations up in this manner was necessary because the interrogating particles could not be biased toward both the HEU and the detector simultaneously. This technique and the use of the ADVANTG code are discussed at length in the first paper in this series [16]. For each of the four steps, the MCNPX simulations were run for 32 h of computer time on 3.4 GHz Xeon processors or for 1×10^{10} source histories, whichever came first.

Once the active background and net HEU signals were determined, Eq. (1) was used to calculate the required source strength of the interrogation source. For this study, the total interrogation time was assumed to be 100 s. The passive background strength was 10 neutrons + 2500 gammas per second. These values were similar to the passive background values found during the validation measurements (See section 5). The significance threshold (z) was set at 5σ above background, making the probability of a false positive due to random statistical variations less than 3×10^{-7} . The source repetition rate was 300 Hz. The ROI extended from the end of one pulse (200 μs) to the beginning of the next pulse, which was at 3.33 ms. Time bins after 3.33 ms were convolved into successive pulses to simulate the buildup of delayed fission neutrons and gammas.

4. Computational results

Figure 3 shows an example of the organic scintillator tally results before the pulse convolution. The cargo is low-density (0.2 g/cm^3) homogeneous iron. The *Void* curve is the active background signal, while the *Total HEU* curve includes the SNM signal as well. The *Net HEU* curve is the difference between the *Total HEU* and *Active Background* curves. There are two main regions where the HEU signal deviates markedly from that of the background. Between the region of about 2 μs and 2 ms, interrogation neutrons dying away in the cargo are inducing fission chains in the HEU, which produce prompt fission neutrons and gammas. These typically decay away with a period of hundreds of microseconds to about a millisecond, depending on the cargo [22]. After approximately 5 ms, the interrogation neutrons have completely died away, and the signal from delayed neutrons produced by fission products is the only remaining signal. Although much weaker than that of the prompt fission neutrons, the delayed neutron signal is a very strong indicator of fissile material if it can be detected. In uranium, the neutron precursors are typically represented by six groups with half-lives ranging from hundreds of milliseconds to nearly a minute [23]. Over many successive pulses, the delayed signal will slowly build up as more and more fissions are induced.

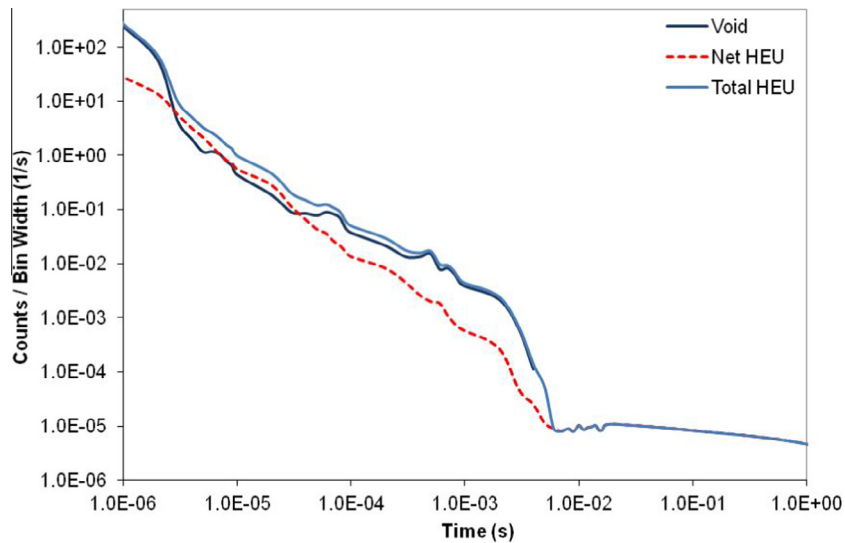


Fig. 3. Example of tally results for an organic scintillator. The cargo is iron at a density of 0.2 g/cm^3 . The detector is an ideal organic scintillator with a 1 MeV neutron energy threshold. Each time bin was normalized on a per-source-neutron basis and divided by its width in seconds.

Figure 4 shows the same type of plot for a ^3He detector. Unlike in Fig. 3, there is no clearly visible distinction between the *Total HEU* and *Active Background* signals in the $2 \mu\text{s}$ and 2 ms region. This is because while the *Net HEU* signal is approximately four times larger than in the scintillator tally results, the *Active Background* is over 100 times greater. This large increase in the background over the scintillator tally is due to the fact that there was no energy threshold for the neutrons, allowing thermal neutrons to be counted.

Figure 5 shows the predicted source strength results for the short axis interrogations where the D–T source and detector are adjacent to the container. In the iron cargo, the fission neutrons are able to pass through the cargo to the detectors fairly easily. This makes the ^3He detectors quite effective, particularly given the low neutron background. The simulations indicate a source strength requirement of about 10^5 neutrons or less for the steel cargo. With the polyethylene and mixed cargos, the hydrogenous material absorbs a large fraction of the neutrons. This results in much higher

source strength requirements, in excess of 10^9 neutrons per second at the highest density. In these cargos, the scintillators require a much lower source strength because they are able to detect the fission gammas in addition to the neutrons. The highest required source strength with a scintillator tally is 10^7 neutrons per second.

Figure 6 shows the results for configuration 2, in which a D–T source was used for an interrogation through five containers of material. The distance and material thickness are approximately equivalent to a lengthwise (12.2 m) interrogation of a cargo container. Even when ADVANTG was used to accelerate the variance reduction, some of the results could not be converged properly for simulations based on 10^{10} source histories. Results in which the total relative error exceeded 50% are unreliable and not shown. The source strength required for the iron cargo is on the order of 10^8 – 10^9 neutrons per second for the ^3He and scintillator results, respectively. At the lowest density, the mixed cargo required over 10^{10} neutrons per second, and polyethylene required more than 10^{13} with the scintillator tallies. Many of the higher density cases

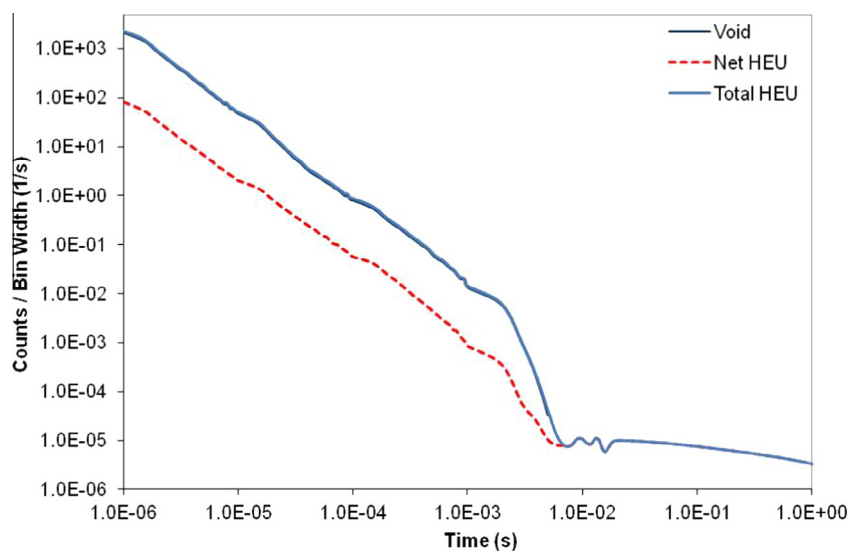


Fig. 4. Example of tally results for a ^3He detector. The cargo is iron at a density of 0.2 g/cm^3 . The detector is an ideal organic scintillator with a 1 MeV neutron energy threshold. Each time bin was normalized on a per-source-neutron basis and divided by its width in seconds.

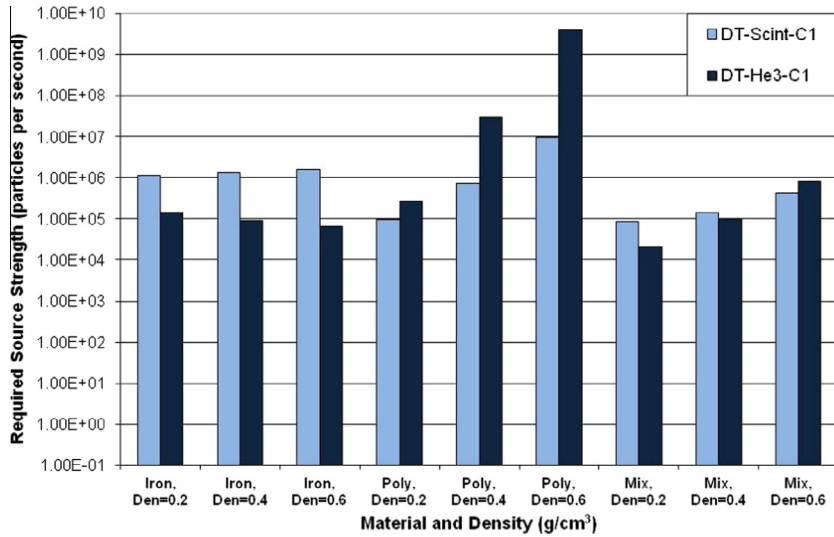


Fig. 5. A comparison of the predicted source strengths required to successfully detect the HEU threat object in various container cargo loadings when the interrogation is performed through the short axis. This chart compares the performance of the idealized ^3He detector and the scintillator when used with a D-T neutron source.

failed to converge, but would undoubtedly require even greater source strengths than the lower density ones.

5. Validation

In 2011–12, a series of measurements were conducted at the Y-12 National Security Complex, in part, to validate the simulation methodology. Because of space limitations within the facility, it was not possible to utilize a standard shipping container. To serve as surrogates for typical cargo container loadings, two customized pallets of shielding material were constructed. The first pallet provides 20" (50.8 cm) of polyethylene shielding around the SNM, and the second 10" (25.4 cm) of steel. These pallets were designed so that the shielding could be reduced by removing 1–2" (2.5 – 5.1 cm) thick layers. For the SNM, an 18 kg annular HEU casting enriched to 93% was used. This casting was fitted with a polyethylene cylinder at the center to increase its neutron multiplication. In this

configuration, the HEU has a bare multiplication value of 2.34. When surrounded by an infinite polyethylene reflector, the multiplication increases to 7.87. The interrogation source was an MP 320 pulsed D-T neutron generator [9]. The generator was operated at an output of $4.64 \times 10^7 \pm 5\%$ neutrons per second. The repetition rate was 300 Hz, and the duty cycle was 6% (200 μs pulse width).

Two arrays of plastic scintillators and two arrays of ^3He detectors were used in the measurements. Liquid scintillators with pulse shape discrimination were not available for these measurements. The plastic scintillators had dimensions of $27 \times 27 \times 9$ cm, and were placed in a 2×2 array. 6" (15.2 cm) of polyethylene shielding was placed between each detector in a cruciform pattern to minimize cross-talk between individual detectors. The neutron energy thresholds of these detectors were measured and found to be 0.75 MeV on average. Each ^3He detector consisted of four 36" (91.4 cm) long by 2" (5.1 cm) diameter tubes of ^3He at 4 atmospheres surrounded by a polyethylene moderator. The moderator

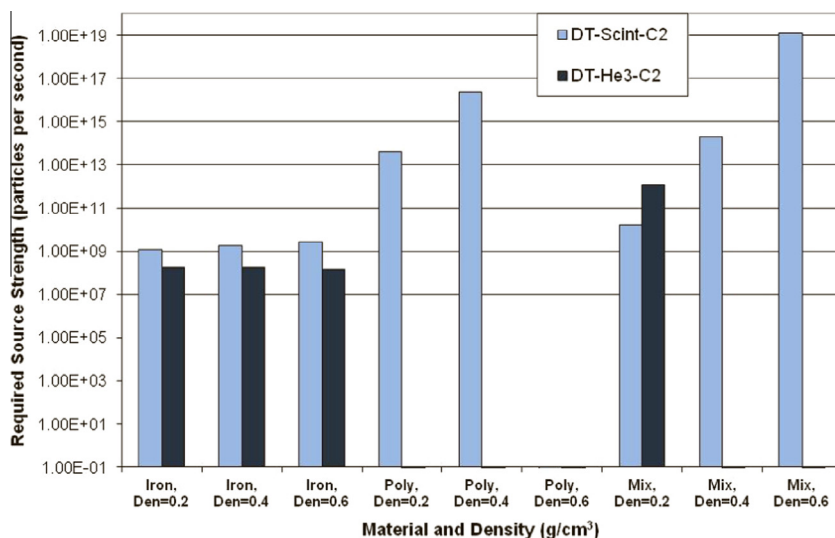


Fig. 6. A comparison of the predicted source strengths required to successfully detect the HEU threat object in various container cargo loadings. The source and detector are separated by approximately 12.2 m. This chart compares the idealized ^3He detector and the scintillator performance when used with a D-T neutron source. Missing values indicate simulations that did not achieve convergence.

was enclosed in BORAL [24] plates to block thermal neutrons from entering the detector. Four of these detectors were stacked vertically to form a ^3He array.

Figure 7 shows the layout of the source, shielding, and detector arrays around the polyethylene shielding (left), and an image of the polyethylene shielding opened up to show the position of the HEU storage casting (right). The steel shielding configuration was similar to that shown in Fig. 7, except that the MP 320 location was moved forward 10" (25.4 cm) so that it was directly against the outside of the steel shielding. The detectors remained in the same position relative to the HEU. Measurements were taken with several thicknesses of steel and polyethylene shielding. Time correlations were measured between the start of the D–T pulse and each of the four arrays of detectors. The average correlations per pulse were integrated in two ROIs, one from 0.5– to 1.0 ms, and the other from 1.0 to 3.0 ms. For each ROI, the SNM signal was computed by subtracting the results of a void measurement from one with the HEU present. The statistical significance of this SNM signal was computed by solving Equation 1 for z .

The two measurements with the full shields (20" polyethylene/10" steel) were simulated using the four-step methodology presented here earlier. The HEU/void measurement times were 94/51 min for the 20" polyethylene shielding and 51/26 min for the 10" steel shielding. The detector arrays were modeled, but the response was limited to current tallies of particles entering the array bodies. For the ^3He arrays, all photons and neutrons below 0.3 eV were ignored to simulate the effect of the BORAL plates. For the scintillator arrays, neutrons below 0.75 MeV and photons below 0.1 MeV were ignored to simulate the discriminator threshold. The statistical significance of the SNM signal was computed in the same manner as for the measurements.

Figs. 8 and 9 show examples of the correlations for both simulations and the measurements. Fig. 8 shows the correlations for the side array of ^3He detectors with 10" of steel shielding, and Fig. 9 shows the correlations for the close array of plastic scintillators with 20" of polyethylene shielding. The ^3He measurements (Fig. 8) show a very distorted shape in the D–T pulse region because the intense neutron flux is saturating the detectors. Because the MCNPX simulations treat each source neutron separately, this shape is not reproduced in the simulations. After the pulse region, the simulated correlations match the shape of the measurements fairly well. The simulations are as much as an order of magnitude larger than the measurements due to the lack of a response function.

Tables 1 and 2 show the statistical significance results for the measurements and simulations in the 0.5–1.0 and 1.0–3.0 ms ROIs, respectively. Those arrays in which the results showed a highly sig-

nificant SNM signal ($z > 5$) are shaded. Both scintillator arrays show a highly significant SNM signal with both shields, while the ^3He arrays fail to show a significant signal with the polyethylene shielding. The measurements and simulations agree with respect to which sets of detector correlations were highly significant in all combinations of detector array, shielding scenario, and ROI. The simulations show a larger z values for all combinations, which is not surprising given that they employ 100% efficient detectors. In the scenarios that showed a statistically significant SNM signal, the simulations overestimate the z value by an average of 2.12, with a maximum of 2.79.

As demonstrated in Equation 2, the required source strength to detect highly shielded SNM scales approximately as the square of the statistical significance. Because the configuration in the validation measurements was somewhat different than what was simulated for the boarded search, the maximum value of 2.79 is used as a conservative estimate. This would indicate that for a given z value, this simulation methodology underpredicts the required source strength by a factor of $2.79^2 = 7.78$. Since this value represents a worst-case difference between the incoming particle fluence and the detector response, its inverse (0.128) also provides a very rough estimate of the intrinsic detector efficiency. This is a reasonable value to be expected for ^3He detectors. For the plastic scintillator arrays, the particle fluence was tallied over the entire detector array, which includes the polyethylene shielding between detectors. Dividing 0.128 by the ratio of the detector surface area to the total surface area of the array suggests an intrinsic efficiency of 0.211. This is somewhat lower than might be expected for a typical fission spectrum; however, the scattering of neutrons and gammas passing through the shielding would result in a larger fraction of particles being near the threshold energy of the scintillator, where the probability of a particle producing a pulse is much lower than at the peak of the fission energy spectrum.

The 7.78 value also represents a scaling term that can be used to adjust the boarded search simulations in Section 4 to estimate the source strength that would be required for the corresponding measurements. Figs. 10 and 11 show the previous computational source strength results scaled by this factor. A horizontal line marks the 4.64×10^7 source strength used in the validation measurements. The results for the short axis interrogation (Fig. 9) indicate that the HEU could be detected using this generator in all of the cargos except for the 0.6 g/cm^3 polyethylene using the plastic scintillator, while the ^3He results exceed the generator strength with the 0.4 and 0.6 g/cm^3 polyethylene cargos. A modest increase in the source strength would make detection in the 0.6 g/cm^3 cargo loading possible with the scintillator. The scaled results for the interrogation through the long axis of the cargo container

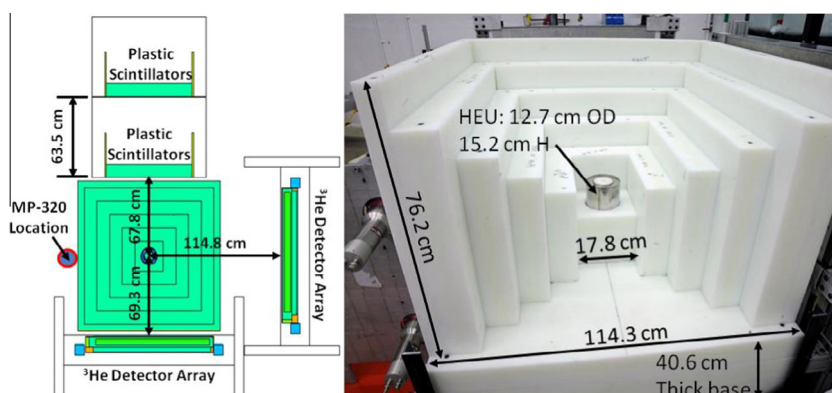


Fig. 7. A cutaway diagram of the measurement configuration (left), and a picture of the polyethylene shielding with one side opened to reveal the location of the HEU casting (right).

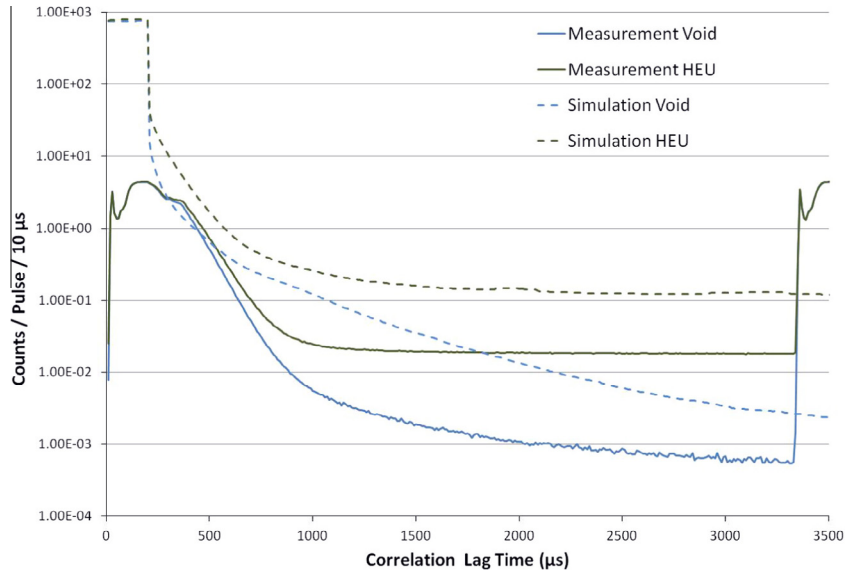


Fig. 8. Time correlations between the MP 320 D-T generator and the side array of ³He detectors with 10" (25.4 cm) of steel shielding. Simulation results are indicated by dashed lines.

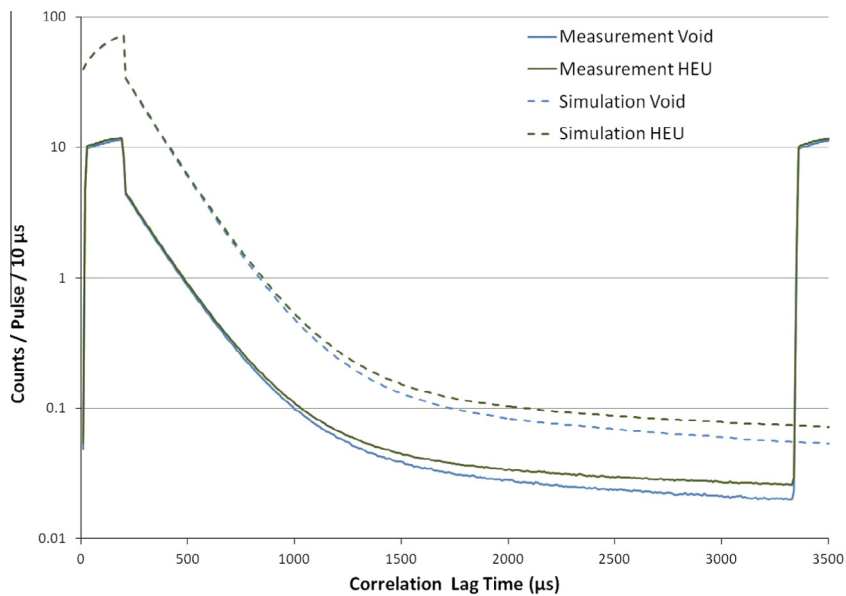


Fig. 9. Time correlations between the MP 320 D-T generator and the near array of plastic scintillators with 20" (50.8 cm) of polyethylene shielding. Simulation results are indicated by dashed lines.

Table 1
Comparison of statistical significance tests between measurements and simulations without response functions for the 0.5–1 ms ROI. Results which indicate a high significance ($Z > 5$) are shaded.

Shielding	Measurements				Simulations			
	He_Back	He_Side	Plast_Close	Plast_Far	He_Back	He_Side	Plast_Close	Plast_Far
20" HDPE	0.9	-2.0	119.9	37.9	0.2	3.1	260.0	82.0
10" Steel	651.0	653.5	349.6	140.7	1172.5	1740.4	662.2	392.8

(Fig. 11) reveal that the HEU would not be detectable for any of the cargo loadings given this source strength.

Note that these results assume that the same detector configurations used in the validation measurement are being used. An

optimization study to determine the best configuration and number of ³He detectors and scintillators could likely improve on these results somewhat. Likewise, employing other detector types, such as a liquid scintillator with PSD might also improve the results.

Table 2

Comparison of statistical significance tests between measurements and simulations without response functions for the 1–3 ms ROI. Results which indicate a high significance ($Z > 5$) are shaded.

Shielding	Measurements				Simulations			
	He_Back	He_Side	Plast_Close	Plast_Far	He_Back	He_Side	Plast_Close	Plast_Far
20" HDPE	1.8	−2.4	255.2	108.9	1.7	0.7	599.6	120.4
10" Steel	1034.1	1594.9	357.5	118.0	2531.2	3735.0	476.9	276.4

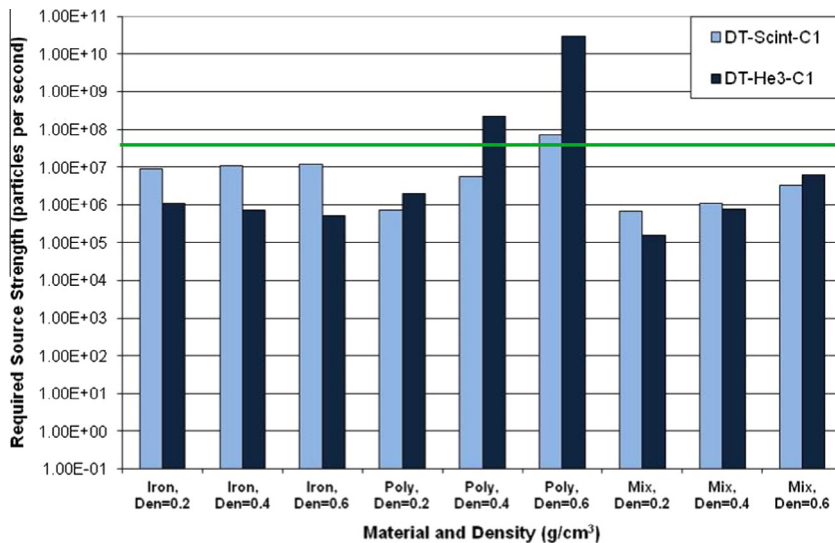


Fig. 10. A comparison of the source strengths required to successfully detect the HEU threat object in various container cargo loadings through the short container axis. The thick horizontal line indicates the source strength of the generator used for the validation measurements.

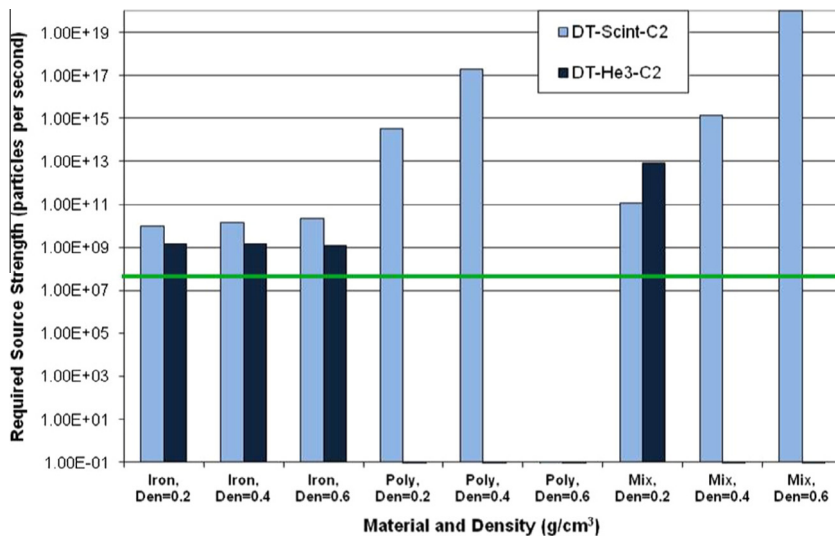


Fig. 11. A comparison of the source strengths required to successfully detect the HEU threat object in various container cargo loadings through the long container axis. The thick horizontal line indicates the source strength of the generator used for the validation measurements. Missing values represent simulations that could not be converged.

6. Conclusions

The possible need for a boarded search of a container ship was shown, and a scenario for the boarding team was presented. Some possible sources and detectors to be used in this search were discussed. An MCNPX model of a container ship carrying 25 kg of HEU was used to simulate the active interrogation. The required source strength to find the HEU was shown for several combinations of detector type, cargo material, and density.

These results were validated using two custom-built pallets of shielding material as surrogates for shipping container cargos. Corresponding measurements and simulations produced correlation curves with similar shapes, although the simulations greatly overestimated the values because they lacked any response functions. At worst, the simulations were found to underestimate the required source strength by a factor of 7.78. This value was used to scale the computational results for the boarded search. These scaled results indicate that a 100 s interrogation with a

4.64×10^7 neutron per second D–T generator can successfully detect the presence of the HEU in homogeneous steel or mixed cargo with a density of up to 0.6 g/cm^3 , and in polyethylene cargo up to a density of 0.4 g/cm^3 . A modest increase in source strength would allow for the detection in polyethylene up to a density of 0.6 g/cm^3 . On the other hand, an interrogation through a block of containers equivalent to the lengthwise interrogation of a 12.2 m container showed that the HEU could not be detected with this source given any of the cargo loadings tested. A substantial improvement in source strength or detector efficiency would be required to make this modality feasible.

Acknowledgments

This research is supported by the National Nuclear Security Administration, Defense Nuclear Nonproliferation, Office of Nonproliferation and Verification Research and Development under contract with UT-Battelle, LLC.

References

- [1] M. Bunn, A. Wier, J.P. Holdren, *Controlling Nuclear Warheads and Materials: A Report Card and Action Plan*, Harvard Univ Press, Cambridge, Mass, 2003.
- [2] C. Meade, R. C. Molander, *Considering the Effects of a Catastrophic Terrorist Attack*, RAND Corporation, Santa Monica, Calif., 2006, http://www.rand.org/content/dam/rand/pubs/technical_reports/2006/RAND_TR391.pdf (Accessed Jan., 2013).
- [3] U.S. Customs and Border Protection, *Container Security Initiative in Summary*, Washington, D. C., 2011, http://www.cbp.gov/linkhandler/cgov/trade/cargo_security/csi/csi_brochure_2011.ctt/csi_brochure_2011.pdf (Accessed Jan., 2013).
- [4] U.S. Customs and Border Protection, *Radiation Portal Monitors Safeguard America from Nuclear Devices and Radiological Materials*, Washington, D. C., 2011, http://www.cbp.gov/xp/cgov/border_security/port_activities/cargo_exam/rad_portal1.xml (Accessed Jan. 2013).
- [5] National Nuclear Security Administration, *Megaports Initiative 2010*, Washington, D. C., 2010, http://nnsa.energy.gov/sites/default/files/nnsa/inlinefiles/singlepages_9-15-2010.pdf (Accessed Jan. 2013).
- [6] V.J. Orphan, E. Muenchau, J. Gormley, R. Richardson, *Advanced γ ray technology for scanning cargo containers*, Nucl. Instrum. Methods 63 (2005) 723–732.
- [7] J.M. Hall et al., *The nuclear car wash: Neutron interrogation of cargo containers to detect hidden SNM*, Nucl. Instrum. Methods B 261 (2007) 337–340.
- [8] J.L. Jones et al., *Detection of shielded nuclear material in a cargo container*, Nucl. Instrum. Methods A 562 (2006) 1085–1088.
- [9] MP 320 Neutron Generator, Thermo Scientific, http://www.thermo.com/eThermo/CMA/PDFs/Product/productPDF_2976.pdf (Accessed Jan., 2013).
- [10] C.E. Moss, M.W. Brener, C.L. Hollas, W.L. Myers, *Portable active interrogation system*, Nucl. Instrum. Methods B 241 (2005) 793–797.
- [11] G.F. Knoll, *Radiation Detection and Measurement*, 3rd Edition., John Wiley & Sons, New York, 2000.
- [12] R.T. Kouzes, E.R. Siciliano, J.H. Ely, P.E. Keller, R.J. McConn, *Passive neutron detection for interdiction of nuclear material at borders*, Nucl. Instrum. Methods A 584 (2008) 383–400.
- [13] U.S. Government Accountability Office, Center for Science, Technology, and Engineering, *Neutron detectors: Alternatives to using helium-3*, GAO-11-753, U.S. Government Accountability Office, Washington, D. C., 2011.
- [14] S.A. Pozzi, J.A. Mullens, J.T. Mihalczko, *Analysis of neutron and photon detection position for the calibration of plastic (BC-420) and liquid (BC-501) scintillators*, Nucl. Instrum. Methods A 524 (2004) 92–101.
- [15] EJ-309, Eljen Technology, <http://www.eljentechnology.com/index.php/products/liquid-scintillators/73-ej-309>, (Accessed May, 2013).
- [16] T. M. Miller, B. W. Patton, B. R. Grogan, J. J. Henkel, B. D. Murphy, J. O. Johnson, J. T. Mihalczko, "Investigations of active interrogation techniques to detect special nuclear material in maritime environments: Standoff interrogation of small- and medium-sized cargo ships", Nucl. Instr. Meth. B (2013), <http://dx.doi.org/10.1016/j.nimb.2013.08.040>.
- [17] U.S. Department of Transportation, Federal Highway Administration, "Commercial Vehicle Size and Weight Program", <http://ops.fhwa.dot.gov/freight/sw/overview/index.htm> (Accessed Jan. 2013).
- [18] T.P. Lou, A. Antolak, *Simulation of Cargo Container Interrogations by D-D Neutrons*, LBNL 61696, Ernest Orlando Lawrence Berkeley National Laboratory, Berkeley, CA, 2007.
- [19] U.S. Congress, Office of Technology Assessment, *Nuclear Safeguards and the International Atomic Energy Agency*, OTA-ISS-615, U.S. Government Printing Office, Washington, D. C., 1995.
- [20] D. Pelowitz (Ed.), *MCNPX User's Manual*, Version 2.6.0, LA-CP-07-1473, Los Alamos National Laboratory, Los Alamos, NM, 2008.
- [21] J.C. Wagner, *An Automated Deterministic Variance Reduction Generator for Monte Carlo Shielding Applications*, Proceedings of the American Nuclear Society 12th Biennial RPSD Topical Meeting, Santa Fe, NM, 2002, April 14–18.
- [22] T. Gozani, *Fission signatures for nuclear material detection*, IEEE Trans. Nucl. Sci. 56 (2009) 736–741.
- [23] J.J. Duderstadt, L.J. Hamilton, *Nuclear Reactor Analysis*, John Wiley & Sons, New York, 1976.
- [24] Ceradyne, Inc. Boron Products, "BORAL", <http://www.ceradyneboron.com/products/nuclear-power/neutron-absorbers/boral/>.